Structural and electronic properties of hydrogen in the potassium-hydrogen-graphite ternary intercalation compound $C_8KH_{0.55}$: A nuclear-magnetic-resonance study

Seiichi Miyajima and Takehiko Chiba
Department of Chemistry, College of Humanities and Sciences, Nihon University, Sakurajosui Setagaya-ku, Tokyo 156, Japan

Toshiaki Enoki and Hiroo Inokuchi
Institute for Molecular Science, Okazaki 444, Japan

Mizuka Sano
Department of Chemistry, Faculty of Science, Kumamoto University, Kumamoto 860, Japan
(Received 4 June 1987)

A proton NMR study was carried out on a second-stage potassium-hydrogen-graphite intercalation compound, C_8KH_x ($x \simeq 0.55$), in a powder form within the temperature range 1.5–77 K. An inhomogeneously broadened NMR signal (around 40 kHz in full width at half maximum) was observed, but the intrinsic linewidth of the spin isochromat, about 3.6 kHz, was determined from the spin-echo envelope. The shape of the echo envelope was explained by assuming a regular two-dimensional structure of dissociated hydride ions. The inhomogeneous broadening may possibly be ascribed to localized electron spins of the order of 100 ppm. The spin-lattice relaxation mechanisms were divided into two contributions, the metallic process and the process due to localized electron spins. Analysis of the metallic relaxation component revealed the existence of a small local density of states at the Fermi level at hydrogen sites, $N(E_F)_H = 0.014$ states per eV per spin per hydrogen atom. The hydrogen atomic plane was revealed to be weakly metallic. A possible electronic structure is discussed.

I. INTRODUCTION

It has been known that gaseous hydrogen is adsorbed in the first-stage graphite-potassium intercalation compound, C_8K, at room temperature.[1,2] This occlusion of hydrogen brings about the change of staging, and gives a new second-stage ternary compound, C_8KH_x ($0.1 \lesssim x \lesssim 0.67$).[3,4] The intercalant in C_8KH_x was revealed to have a sandwich structure of triple atomic planes, K-H-K, along the c axis,[5–7] in which the hydrogen atomic plane is negatively charged due to the strong electron affinity of hydrogen,[8–13] whereas the potassium atomic planes are positively charged. A problem occurred about the chemical species of hydrogen since Conard *et al.* reported that they could not observe the proton NMR signal of C_8KH_x ($x = \frac{2}{3}$).[8] They tried to explain the absence of a proton signal by assuming that the gaseous hydrogen adsorbed in the intercalant layer was not dissociated into H^- ions but became H_2^- species, and that the proton signal was smeared out due to the strong hyperfine field of the magnetic H_2^- ion. It was also known, however, that the H-D exchange reaction was catalyzed by C_8K,[14] which proved that molecular hydrogen was once dissociated and recombined in some stages of the adsorption-desorption cycle. A neutron scattering study was carried out by Trewern *et al.*,[15,16] and a possible in-plane structure of hydrogen was proposed, which consisted of a unit cell having a $(2\times\sqrt{3})R(0°,30°)$ rectangular superlattice with respect to the unit translational vectors of hexagonal graphite. However, it was still in question whether H^- or H_2^- was the constituent unit. The first motive of the present work is thus to clarify the chemical species and the in-plane order of hydrogen in C_8KH_x.

The electronic properties of this compound have been extensively studied by Enoki and his colleagues from experiments by ESR,[9,10] positron annihilation,[11] specific heat,[12] and the Schubnikov–de Haas effect.[13] It has been pointed out[12,13] that C_8KH_x has an intermediate electronic character between the transition-metal hydrides, which are regarded as alloys, and the alkaline hydrides, which are ionic insulators. Schematically speaking, the electric conduction is mainly ascribed to the metallic graphite layers separated by the insulating K^+-H^--K^+ ionic intercalants. The 1s-like band originating from hydrogen was assumed to lie well below the Fermi level, and have a localized electronic character. However, there has been no clear evidence that the hydrogen layer is really insulating. We therefore tried to extract information on the electronic properties of this hydrogen layer by the NMR technique, and show a possible electronic structure of $C_8KH_{0.55}$.

This paper analyzes the NMR line shape, and shows that hydrogen dissociated into monatomic ions forms a two-dimensional rigid lattice. It is also suggested that a small amount of localized electron spins is present. The spin-lattice relaxation data show that there is a small but nonzero amount of carrier density at the hydrogen nucleus. A plausible electronic structure of C_8KH_x is proposed.

II. EXPERIMENT

The sample of C_8K was prepared from Grafoil GTA (Union Carbide Co.) and potassium metal because it was known that hydrogen absorption took place homogeneously in Grafoil-based C_8K, but inhomogeneously in a sample based on well-oriented graphite.[17] After Grafoil was ground into 36-mesh powder and potassium was vacuum distilled three times, they were sealed in a glass tube under vacuum. The reaction was carried out at 260 °C for a week, following the procedure described by Nixon and Parry.[18] Hydrogen gas purified by passing through a Pd-Ag thimble heated to 450 °C was then introduced into the C_8K at room temperature. The amount of adsorbed hydrogen was measured *in situ* from the change in hydrogen pressure. The final amount, $x=0.55$, was achieved after a week. The sample, weighing 0.2 g, was then sealed in a Pyrex tube with the hydrogen gas at 93 kPa.

A pulsed NMR apparatus was constructed for this experiment. The radio frequency from an HP-3335A oscillator was modulated by a homemade transistor-transistor-logic pulse programmer, and amplified by Matec 515A/525 power amplifiers. The highest Larmor frequency in this study was 55 MHz, which was limited by the capability of a Varian V-7300 electromagnet. A Clark-McNeil type matching network[19] was used. The receiver consisted of Matec 254 and 625 amplifiers and a R&K PS-2C wideband phase shifter. The receiver system was totally broadbanded. The signal was recorded by using a transient recorder, Kawasaki M-500T, and a signal averager, TMC-400. The recovery time was 4 μs at 55 MHz, and 8–10 μs at 20 and 7 MHz. The pulse sequence, 90° comb-τ_1-90°-τ_2-180°-τ_3-, was used. The spin echo envelope was observed by varying τ_2, and the spin-lattice relaxation rate was measured by changing τ_1.

A copper-shielded sample cavity was set in a stainless steel cryostat. Temperature control was achieved in the temperature range between 4.2 and 77 K by means of a continuous-liquid helium-flow system equipped with a small vacuum pump and a proportional controller. The temperature was controlled to well within 1 K throughout the experiment. A calibrated germanium resistor (Lake Shore Cryogenics, Inc.) and thermocouples of Au+0.07 at. % Fe versus Chromel (Osaka Sanso Kogyo Ltd.) were used to measure the temperature below and above 4.2 K, respectively.

III. RESULTS AND DISCUSSION

A. General features of the NMR line

Proton NMR signals were detected in free decays and spin echoes. Figure 1 shows the spin echo observed at 4.2 K. As is seen from Fig. 1, the apparent phase memory time (T_2^*) was ca. 8 μs, but the spin echo was found to have a long envelope when measured by varying τ_2. The envelope of the echo height measured at 4.2 K is plotted in Fig. 2. Although precise measurement of the echo height was difficult in the short τ_2 region ($\tau_2 \lesssim 20$ μs) because of the overlap between the free decay and its echo induction, the line shape was found to be close to Lorentzian in the long-τ_2 region. If the characteristic decay time of the spin echo envelope is represented by T_2', the T_2' was estimated to be 90 μs, and the Lorentzian fit with $T_2'=90$ μs ($\Delta\nu=1/\pi T_2'=3.6$ kHz) is drawn in Fig. 2. The fact that T_2' is greater by an order of magnitude than T_2^* indicates that the apparent NMR linewidth (ca. 40 kHz) is determined by an inhomogeneous broadening brought into the proton spin system from an external system, and that the intrinsic time-domain spectrum of the spin isochromat is obtained in the echo envelope.

Neither T_2^* nor T_2' exhibited appreciable temperature dependence below 40 K, showing that neither inhomogeneous nor homogeneous broadening is affected by motional narrowing. Hydrogen species are not liquidlike but are fixed around their lattice points below 40 K. Quantitative analysis of line shape was difficult above 40 K because of poor signal-to-noise ratio.

We now consider why the proton NMR signal is so weak. One of the possible explanations for this phenomenon may be the existence of molecular hydrogen. The ground state of molecular hydrogen is the

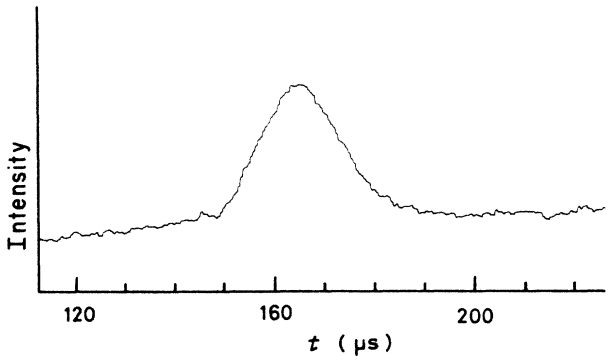

FIG. 1. Proton spin echo of $C_8KH_{0.55}$ observed at 4.2 K and 20 MHz. The pulse sequence, 90° comb-τ_1-90°-τ_2-180°-τ_3-, was applied with $\tau_1=225$ s, $\tau_2=80$ μs, and $\tau_3=100$ ms. The echo was accumulated eight times. The origin of time on the figure is the time of onset of the central 90° pulse.

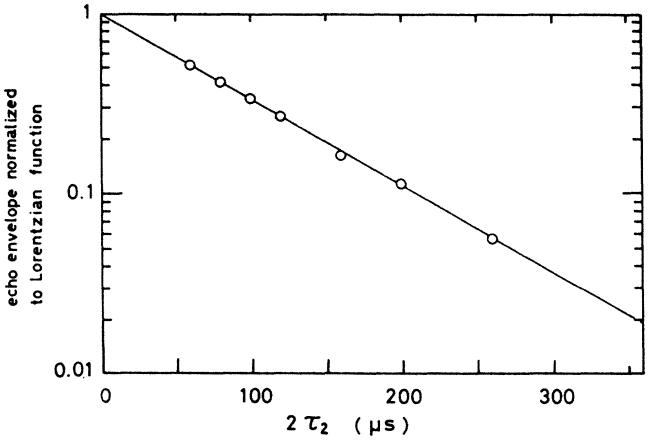

FIG. 2. Proton spin echo envelope observed at 4.2 K and 20 MHz. The echo envelope is normalized to Lorentzian with $T_2'=90$ μs.

spin-singlet state (parahydrogen) which does not give a NMR transition. So, the signal intensity is reduced according to the ratio of these species. If it is the case, the characteristic dipolar doublet structure will be generated by the ortho species at low temperatures where internal motion of the molecule is frozen. Another noticeable feature of this case is that the signal intensity will change gradually after the temperature is stepped up or down, and the equiliburium intensity will exhibit unusual temperature dependence, with the weaker signal in the lower temperature, because the ortho-para conversion rate is expected to be in an observable order of magnitude.[20,21] In our experiment, however, neither time evolution nor anomalous temperature dependence of the signal intensity was detected in addition to the absence of the characteristic doublet structure. So, it will be natural to conclude that the adsorbed hydrogen molecules are dissociated into monatomic species and are fixed at the lattice points within the intercalant layer. The fact that neither motional narrowing of the line nor motional contribution to T_1^{-1} were detected is an additional support to this conclusion. The weakness of the proton signal must therefore be attributed to some other origin.

Another possible explanation for the weakness of the proton signal is associated with the observed inhomogeneous broadening of the line. In order to elucidate such inhomogeneous broadening in our experiment and also the absence of a proton signal in Conard's experiment,[8] we now think about the lattice structure of hydrogen in C_8KH_x. Although there is no conclusive picture for hydrogen structure in C_8KH_x, a possible model was proposed by Trewern *et al.*[15] This model [Fig. 3(a)] assumes that the potassium atoms are arranged in a $(2\times2)R(0°)$ hexagonal in-plane superlattice with respect to the unit translational vectors, $\mathbf{a}_G$ and $\mathbf{b}_G$, of hexagonal graphite ($a_G=2.46$ Å), and the two potassium lattices constituting the unit of K-H-K sandwich intercalant are shifted from each other by one unit length (a_G) along the a axis of graphite. The two potassium atomic planes provide tetrahedral voids for hydrogen. According to Trewern *et al.*, half of the tetrahedral voids are filled with hydrogen, and the $(2\times\sqrt{3})R(0°,30°)$ rectangular superlattice is formed. Since we know that hydrogen molecules are dissociated into monatomic anions, this structure leads to a hydrogen content, $x=0.5$. A question about this structure may be why the hydride ions do not form a hexagonal closest-packing structure. An alternative model is therefore proposed here, which is the $(2\times2)R(0°)$ hexagonal structure of hydride ions sketched in Fig. 3(b). In this model (b), hydrogen content is the same as (a). Because hydride ions form a two-dimensional hexagonal closest-packing structure, this will be the most fundamental structure as a starting model for the ionic intercalants. The shortest H—H distance is 4.26 Å in the rectangular lattice model, and 4.92 Å in the hexagonal lattice model. When adsorbed hydrogen exceeds $x=0.5$, the hydride ions additionally occupy the tetrahedral interstitials which do not accommodate hydride ions at lower hydrogen concentrations ($x\leq0.5$) in either of the lattice models. Around these excess hydride ions, the shortest H—H distance becomes 2.46 Å, which is considerably less than 4.16 Å, the diameter of a H^- ion.[22] So, the introduction of a larger amount of hydrogen than $x=0.5$ will distort the local lattice, and some kinds of defect structure will be generated around this excess hydrogen. One of the possible situations happening to the excess hydrogen may be deviation from the two-dimensional structure, where adjacent hydride ions are shifted up and down from each other. Another possibility may be formation of some other chemical species: paramagnetic species, H_2^- or atomic hydrogen, are among the candidates of such species. This will be one of the reasons why it is difficult to intercalate large excess of hydrogen atoms, and also why the proton NMR results are so strongly dependent on samples. If paramagnetic species are present, the proton signal is inhomogeneously broadened, and part of the signal is wiped out due to the strong local field generated by the Curie spin. This will be the reason why the NMR signal is so broad and weak in our specimen and why the signal totally escaped from observation in Conard's case. Quantitative analysis will be given in Sec. III C.

Recently a large rectangular superlattice, $2\sqrt{3}\times5$, was reported by Guerard *et al.*,[23] for a compound $C_8KH_{0.8}$

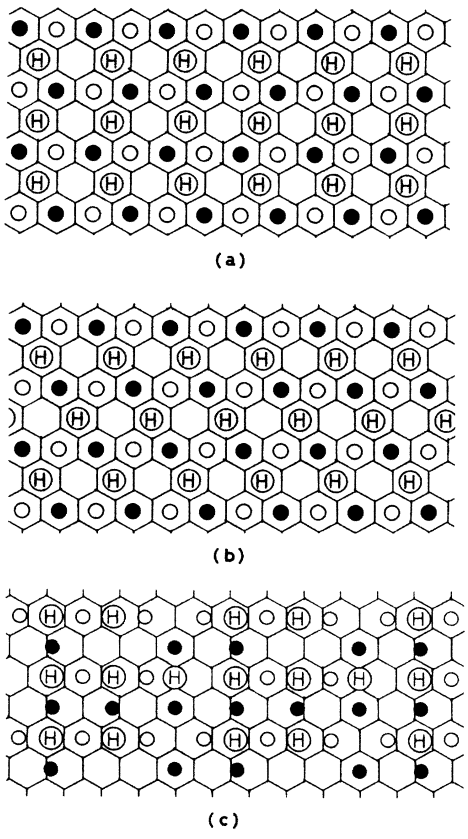

FIG. 3. Structural models of second stage $C_8KH_{0.5}$. The stacking order along the c axis is -C(A)-C(B)-K(○)-H-K(●)-C(B)-C(A)-. The honeycomb network represents the hexagonal C(B) graphite lattice. The three structural models correspond respectively to (a), $(2\times\sqrt{3})R(0°,30°)$; (b), $(2\times2)R(0°)$; and (c), $(2\sqrt{3}\times5)R(0°,30°)$ in-plane superlattice models of hydrogen structure.

prepared through direct intercalation of potassium hydride into oriented graphite. Very recent experiment on neutron scattering[24] also supported this structure. Considering that the hydrogen content ($x=0.8$) is much greater than the limiting value ($x=0.67$) prepared through hydrogen chemisorption, the structure of this compound may be different from ours. The proposed structure itself is very interesting. By applying the $2\sqrt{3}\times 5$ superlattice suggested by Kamitakahara,[24] a tentative model of $C_8KH_{0.5}$ is shown in Fig. 3(c), in which the hydrogen lattice has $\frac{1}{6}$ vacancies and the shortest H—H distance is 4.10 Å. According to this model, hydrogen atoms exceeding $x=0.5$ will be able to be accommodated in the vacancies to $x=0.6$, and introduction of more hydrogen will require additional sites in the interstitials of the hydrogen lattice, so that the excess hydrogen atoms will have the shortest H—H distance of 2.96 Å from the surrounding hydrogen atoms.

B. Line-broadening due to nuclear dipolar interactions

We now calculate the NMR line shape in a more quantitative manner. The decay time of the spin-echo envelope, T_2', is generally described as the sum of the two terms,

$$T_2'^{-1}=T_1^{-1}+T_2^{-1}\ , \tag{1}$$

where T_1^{-1} and T_2^{-1} are the spin-lattice and the spin-spin relaxation rates, respectively. But one can rewrite Eq. (1) as

$$T_2'^{-1}=T_2^{-1}\ , \tag{2}$$

because $T_2^{-1}\gg T_1^{-1}$ is always satisfied throughout the experiment. The overwhelming contribution to T_2^{-1} is the magnetic dipole-dipole interaction among the proton spins. The contributions from the other magnetic nuclei are neglected. The effect of conduction electrons on the line broadening is also neglected because the carrier density is very small in the hydrogen atomic plane, as will be proved in Sec. III D. So the time-domain spectrum is calculated on the basis of dipole-dipole interactions among the protons arranged in the crystal. Although the hydrogen content is 0.55 in the present specimen, the local structure around the excess (0.05) hydrogen is difficult to be treated quantitatively in the three structure models shown in Fig. 3 because of possible distortion of the lattice. Therefore, it suffices to calculate the NMR line shapes in the case of $x=0.5$ for simplicity, and compare them with the experiment.

The spin echo envelope, $G(t)$, can be calculated by the progression[25,26]

$$G(t)=\sum_n (-1)^n\frac{\langle\Delta\omega^{2n}\rangle t^{2n}}{(2n)!},\quad n=0,1,2,\ldots \tag{3}$$

where $\langle\Delta\omega^{2n}\rangle$ is the $2n$th moment of the line, which is calculated by taking the lattice sum of dipole-dipole interactions among the protons. Because all the protons are crystallographically equivalent in either of the two models (a) and (b) of Fig. 3, the lattice sum is taken from the proton located at the origin to the proton located at $\mathbf{r}_{hk}$ where h and k are two-dimensional lattice indices along a and b axes, respectively. The second moment is then given by Van Vleck's formula,[27]

$$\langle\Delta\omega^2\rangle=3\gamma_n^4\hbar^2I(I+1)\sum_h\sum_k r_{hk}^{-6}[p_2(\cos\theta_{hk})]^2\ , \tag{4}$$

where $p_2(x)=\frac{1}{2}(3x^2-1)$ is the Legendre polynomial of rank two, and θ_{hk} is the angle between the vector $\mathbf{r}_{hk}$ and the external magnetic field. Let us first consider the case of an oriented crystal which has the well-defined c axis, but is polycrystalline within the ab plane. In this case, the dipole sum is averaged out within the ab plane and gives the equations

$$\langle\Delta\omega^2\rangle=Af(\theta_0)\sum_h\sum_k r_{hk}^{-6}\ , \tag{5}$$

$$A=3\gamma_n^4\hbar^2I(I+1)\ , \tag{6}$$

$$f(\theta_0)=\tfrac{1}{32}(27\cos^4\theta_0-30\cos^2\theta_0+11)\ . \tag{7}$$

These equations predict that the NMR line becomes narrowest when the c axis of the crystal is tilted by $\theta_0=41.8°$ from the external magnetic field, where the second moment takes a value about $\frac{1}{4}$ times as small as that obtained at $\theta_0=90°$. The radial factor ($\sum_h\sum_k r_{hk}^{-6}$) is calculated to be $0.1211a_G^{-6}$ and $0.0996a_G^{-6}$ for the rectangular and hexagonal $C_8KH_{0.5}$, respectively.

Although Eq. (3) gives the rigorous calculation of $G(t)$, the Gaussian approximation will be a reasonable simplification in the present case, where the in-plane symmetries are high and the number of interacting spins are large. The θ_0-dependent echo envelope, $G(\theta_0,t)$, is thus represented by

$$G(\theta_0,t)=\exp(-\tfrac{1}{2}Af(\theta_0)\sum_h\sum_k r_{hk}^{-6}t^2)\ , \tag{8}$$

and the powder pattern of the envelope, $G_p(t)$, is given by averaging Eq. (8) with respect to θ_0, i.e.,

$$G_p(t)=\tfrac{1}{2}\int_0^{\pi}\exp\left[-\tfrac{1}{2}Af(\theta_0)\sum_h\sum_k r_{hk}^{-6}t^2\right]\sin\theta_0 d\theta_0\ . \tag{9}$$

The $G_p(t)$ are calculated for the rectangular and hexagonal superlattice models, and are represented in Fig. 4 together with the experimental data at 4.2 K. Since the precise value of $G_p(0)$ cannot be known from the experiment, the experimental data are normalized to the calculated curves at $t(=2\tau_2)=60$ μs. It is seen that either of the two models can reproduce the data fairly well. Figure 4 shows that the hexagonal $(2\times 2)R(0°)$ lattice model is a little more satisfactory than the rectangular $(2\times\sqrt{3})R(0°,30°)$ lattice model. This is consistent with the recent report of a transmission-electron-microscopy experiment on the second stage C_8KH_x.[7] However, our NMR study is not enough to finally decide the hydrogen structure, taking into account the approximation that the hydrogen concentration is assumed to be $x=0.5$ whereas the actual concentration is $x=0.55$, and the experimental limitation that only the powder pattern was obtained. Anyway, it is concluded that the experimental echo en-

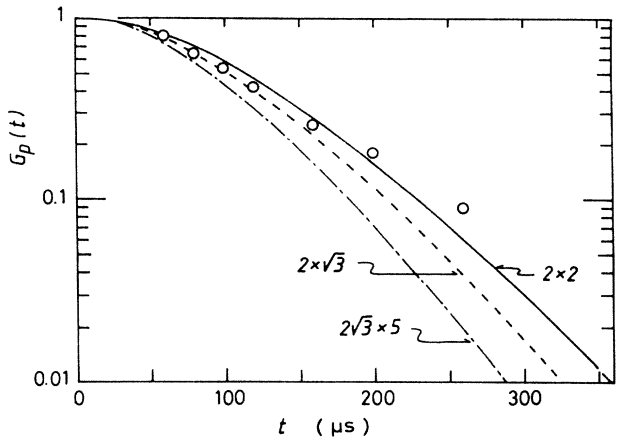

FIG. 4. Comparison of the experimental spin echo envelope with the calculated spectra. The solid and the dashed lines are the calculated $G_p(t)$ based on $(2\times2)R(0°)$ and $(2\times\sqrt{3})R(0°,30°)$ lattice models, respectively. The dash-dotted line represents the result of the $(2\sqrt{3}\times5)R(0°,30°)$ lattice model.

velope can be explained by the two-dimensional static structure of hydrogen atoms.

The calculated envelope assuming the $(2\sqrt{3}\times5)R(0°,30°)$ superlattice is also shown in Fig. 4. Agreement with the experimental data is less satisfactory.

C. Inhomogeneous broadening due to localized electron spins

We now discuss the inhomogeneous broadening observed in free precessions and spin echoes. As the origin of this broadening is not clearly understood yet, we make here a tentative estimate of the effect of localized electron spins associated with the defect structure of the hydrogen lattice. In our models of the hydrogen lattice shown in Fig. 3, hydrogen atoms exceeding $x=0.5$ are accommodated in interstitials of the regular hydrogen lattices accompanied by local distortion of the lattices. It is assumed that some of these excess hydrogen atoms become paramagnetic centers, and generate inhomogeneous linewidths in the NMR lines, depending on the distances between the center and the hydrogen nuclei. The inhomogeneously broadened time-domain spectrum is calculated by the equation

$$I_p(t)=\frac{1}{2N}\int_0^{\pi}\sum_h\sum_k\exp\left[-\tfrac{1}{2}A'f(\theta_0)\sum_{h'}\sum_{k'}r_{hkh'k'}^{-6}t^2\right]\times\sin\theta_0 d\theta_0\ , \tag{10}$$

and

$$A'=\tfrac{4}{3}\gamma_n^2\gamma_e^2\hbar^2S(S+1)\ . \tag{11}$$

Here, $r_{hkh'k'}$ is the distance between the electronic (S) and the nuclear (I) spins when they are located at the lattice points, $\mathbf{r}_{h'k'}$, and $\mathbf{r}_{hk}$, respectively. N is the number of interacting nuclear spins taken into lattice sum. In Eq. (10), the powder average and similar approximations are adopted as in the previous section. Although the electron spins may be expected to be randomly distributed in the crystal, we assumed for simplicity that they are distributed regularly, making a superlattice with respect to the hydrogen $(2\times\sqrt{3})R(0°,30°)$ lattice, and the results are shown in Fig. 5 for various concentrations. Figure 5 shows that the concentration of S spin is 200–300 ppm relative to the I spins in our specimen. The disagreement that the observed peak at $t=0$ is rounded in comparison with the calculated curves is due to the experimental limitation that the rf pulses have nonzero widths.

The concentrations of S spin estimated from the inhomogeneous broadening suggests 0.2–0.3 % of the excess hydrogen atoms contribute to the localized electron spins. It will be natural to assume that a small number of molecular anions, H_2^-, or atomic hydrogen species are generated, since the interionic distances are very short around the excess hydride ions as mentioned in Sec. III A, and electrons are a little too dilute to make hydride ions with a complete valence of -1 (see next section). One can also note from Fig. 5 that it will be difficult to observe the NMR signal if the S spin concentration amounts to ca. 1000 ppm, because in such a case T_2^* becomes close to the width of the 90° pulse. It may have been the case in the experiment by Conard *et al.*[8] because the hydrogen content was reported to be $x=\frac{2}{3}$ in their experiment, which means that their sample contained three times as much excess hydrogen as our sample. On the contrary, the inhomogeneous broadening will

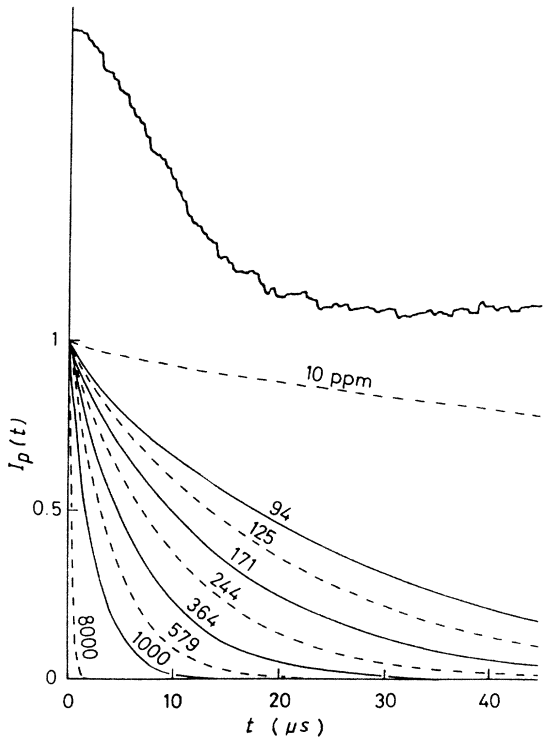

FIG. 5. Comparison of the experimental spin echo with the calculated spectra. The upper trace is the latter half of the experimental spin echo observed at 4.2 K: The lower traces show the calculated inhomogeneous broadenings, $I_p(t)$, for various concentrations of S spins.

be negligible if the S/I ratio is of the order of 10 ppm or less. In fact, we were recently informed that a fairly homogeneous NMR line was observed in C_8KH_x by Nomura *et al.*[28] Their specimen was prepared by reaction between hydrogen gas and HOPG based C_8K at high temperature (240 °C). It is of interest to note the difference in host material [Grafoil and highly oriented pyrolytic graphite (HOPG)] and the difference in reaction conditions (room temperature and high temperature) between our specimen and that of Nomura *et al.*

On the other hand, another completely different explanation may be possible for the inhomogeneous broadening of our sample because the existence of extrinsic magnetic impurity was suggested by Kobayashi in his recent measurement of static susceptibility of Grafoil.[29] It is said that a small amount of iron can possibly be incorporated during the manufacturing process of Grafoil. According to Kobayashi, the concentration was estimated to be 200 ppm relative to the number of carbon atoms from the low-temperature data of the susceptibility. If this estimate is correct, this extrinsic impurity can also be the origin of the inhomogeneous broadening. Therefore it seems difficult to decide, from our experiments only, whether the broadening is due to paramagnetic centers generated on the hydrogen lattice or due to extrinsic impurities. However, let us now be reminded of some other experimental results. Conard *et al.* could not observe the proton signal in $C_8KH_{2/3}$ prepared from powder graphite, which is expected to be free from extrinsic magnetic impurities.[8] According to the recent report by Guerard *et al.*,[23] the proton signal was hardly detectable in potassium-hydrogen-graphite intercalation compounds, whereas clear signals were detected in sodium-hydrogen-graphite compounds prepared from the common material of oriented graphite. These experimental facts support the picture that the observed inhomogeneous broadening comes from the intrinsic nature of the hydrogen species in C_8KH_x. In this section we presented a possible explanation for this broadening, but it is to be noted that the nature of this broadening is not fully understood yet.

D. Metallic contribution to spin-lattice relaxation

The spin-lattice relaxation behavior at 4.2 K is shown in Fig. 6. A nearly exponential relaxation was observed within experimental error throughout our experiment. We saw in the previous section that the NMR line is inhomogeneously broadened up to ca. 40 kHz, but this exponential spin-lattice relaxation proves that the spin diffusion is effective among the nuclei which are subject to different local magnetic fields. So, the spin-temperature concept is valid in this compound, and the well-defined T_1^{-1} was determined from the experiment. Figure 7 represents the entire data set of T_1^{-1}. T_1^{-1} is divided into two contributions according to their temperature dependences: the term which is proportional to temperature, and the term independent of temperature. The former, T_{1m}^{-1}, is attributable to a metallic mechanism, and the latter, T_{1l}^{-1}, is due to localized electron spins, i.e.,

$$T_1^{-1}=T_{1m}^{-1}+T_{1l}^{-1} . \tag{12}$$

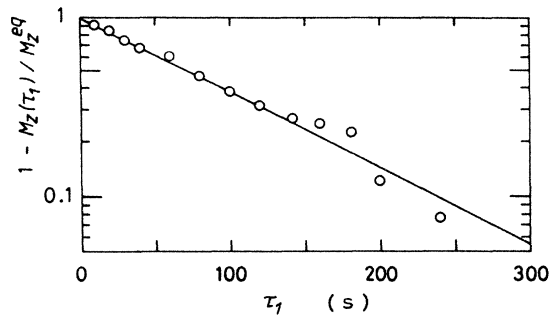

FIG. 6. The z-axis magnetization (M_z) recovery observed at 4.2 K and 55 MHz.

Both terms are insensitive to the NMR frequency. The best fit to the 55-MHz data revealed that $(T_{1m}T)^{-1}=2.9\times10^{-4}\ \mathrm{s^{-1}K^{-1}}$ and $T_{1l}^{-1}=9.0\times10^{-3}\ \mathrm{s^{-1}}$. We now center attention upon the metallic term first.

The hydrogen atomic plane has been assumed to be insulating according to the existing band picture of C_8KH_x,[12] in which the energy band associated with the hydrogen $1s$ level is completely filled because of the strong electron affinity of hydrogen. However, our observation that the metallic term contributes to proton relaxation reveals the existence of charge carriers at the hydrogen site which are generated on a partially filled band. This metallic electronic state of hydrogen was also reported in a very recent paper by Nomura *et al.*[28] A question is what the nature of this partially filled band is. The metallic nature of hydrogen in crystal has been known in transition-metal hydrides, e.g., VH_x (Ref. 30) and TiH_x,[31] in which the hydrogen $1s$ atomic orbital is hybridized with part of the d orbitals originating from transition metals, and forms a partially filled band. Therefore, due to their electronic character, these com-

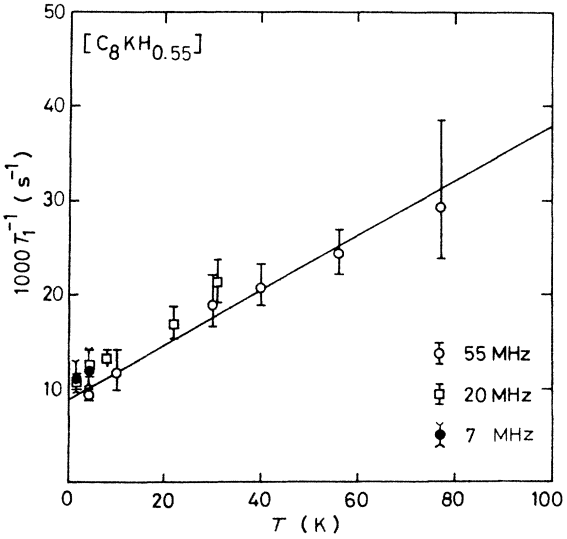

FIG. 7. Temperature and frequency dependences of spin-lattice relaxation rates. The experimental data, ●, □, and ○, stand for 7, 20, and 55 MHz, respectively. The solid line represents the best-fit linear function for the 55-MHz data.

pounds are described as metal-hydrogen alloys, and the proton spin-lattice relaxation is divided into pure Fermi contact, core-polarization, and orbital contributions. In the present compound, however, the only band which can possibly be mixed with the hydrogen 1s orbital is the band originating from the potassium 4s orbital, because the carbon atoms are segregated from hydrogen due to the sandwich stacking, K-H-K, of the intercalant atomic planes. We can therefore assume that the electronic wave function which affects the proton relaxation is essentially of s character, and treat the spin-lattice relaxation in the context of pure contact interaction. The T_{1m}^{-1} is represented by[32]

$$T_{1m}^{-1}=4\pi k_B T\hbar^{-1}[\gamma_n\hbar B_{\rm hf}N_{\rm H}(E_F)]^2 , \tag{13}$$

where $B_{\rm hf}$ is the intensity of the hyperfine field at the nucleus, and $N_{\rm H}(E_F)$ is the local electronic density of states at the hydrogen site per unit energy per one direction of electron spin per atom of hydrogen. The hyperfine field is calculated by the equation,

$$B_{\rm hf}=\frac{4\pi}{3}\gamma_e\hbar\langle\,|\psi_{\mathbf{k}}(0)|^2\rangle_{E_F} . \tag{14}$$

Here, $\psi_{\mathbf{k}}(r)$ is the Bloch function of the s-like conduction electron, and $\langle\,|\psi_{\mathbf{k}}(0)|^2\rangle_{E_F}$ is the expectation value of $|\psi_{\mathbf{k}}(\mathbf{r})|^2$ populated on the Fermi surface at the position of a proton. By applying the experimental value of $(T_{1m}T)^{-1}$ to Eq. (13), one obtains $\gamma_n\hbar B_{\rm hf}N_{\rm H}(E_F)=1.33\times10^{-8}$ states per spin per hydrogen atom. Because our goal in this treatment is to obtain the value of $N_{\rm H}(E_F)$, the intensity of the hyperfine field must be calculated from the nature of the hydrogen wave function. Although it is difficult to solve this problem from the NMR experiment only, a recent experiment on thermoelectric power[33] gave us a clue to the solution: A small hole band was shown to coexist with a large electron band on the Fermi surfaces of C_4KH_x and C_8KH_x.[33] It is surely concluded that the large electron band has the character mainly of the antibonding π^* band of graphite. The additional small hole band is attributable to the almost filled 1s band of hydrogen, in which electrons are a little too dilute to form a completely filled $1s^2$ (i.e., H^-) configuration. The experiment on thermoelectric power showed the character of the carrier, whereas the NMR experiment found that the carrier density was populated at the site of hydrogen nucleus. Smallness of the cross section on the Fermi surface of this hole band[33] (two orders of magnitude smaller than that of the electron band) is consistent with the smallness of the metallic relaxation component in our experiment. The value of $(T_{1m}T)^{-1}$ in this compound is one or two orders of magnitude smaller than that of transition-metal hydrides.[30,31] The observed Korringa term is therefore concluded to come from a hole in the almost filled 1s band of hydrogen, and mixing of the 4s and 1s bands can be neglected. One of the simplest approximations for this hydrogen wave function is the Slater-type 1s orbital,

$$\psi(\mathbf{r})=\left[\frac{Z_e^3}{\pi a_0^3}\right]^{1/2}\exp\left[-\frac{Z_e r}{a_0}\right] , \tag{15}$$

where a_0 is the Bohr radius, and Z_e is the effective nuclear charge screened by the other electron. By taking the screening constant $\sigma=0.3125$ for the $1s^2$ configuration from the numerical table of Clementi *et al.*,[34] $|\psi(0)|^2=6.98\times10^{23}$ cm^{-3} is obtained. If the quantity $\langle\,|\psi_{\mathbf{k}}(0)|^2\rangle_{E_F}$ in Eq. (14) is now replaced by $|\psi(0)|^2$, the local density of states at the hydrogen site is estimated to be $N_{\rm H}(E_F)=0.014$ states eV^{-1} per spin per hydrogen atom. The approximations in this treatment is that we employed the 1s wave function in free space instead of the periodic Bloch functions in addition to the fact that Slater orbital is in itself an approximate function.

Enoki *et al.*[12] obtained the total density of states $N(E_F)$ from the low-temperature specific heat measurements in C_8KH_x with several different hydrogen contents, and showed that $N(E_F)$ decreases almost linearly as hydrogen content increases. Interpolation of the $N(E_F)$-versus-x relation at $x=0.55$ gives the estimation that $N(E_F)=0.11$ states eV^{-1} per spin per carbon atom. The ratio of the local density of states at the hydrogen site to the total density of states is now calculated to be $N_{\rm H}(E_F)/N(E_F)=0.009$ for $C_8KH_{0.55}$. This finding means that the charge carriers on hydrogen sites play a minor role in the transport phenomena of this compound, and that the overwhelming majority of the carriers are associated with the graphite π^* band and possibly with the potassium 4s band.

Taking into account these experimental results and analyses, we can illustrate in Fig. 8 a schematic picture of the electronic structure of $C_8KH_{0.55}$. Figure 8(a) shows $N(E)$ of C_8K, which is a typical donor-type graphite in-

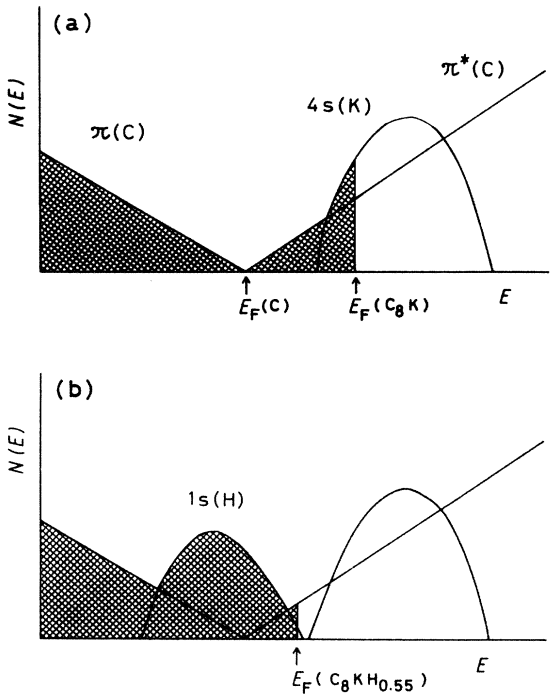

FIG. 8. Schematic illustrations of the electronic density of states of (a) C_8K and (b) $C_8KH_{0.55}$.

tercalation compound. The amount of charge transfer from the potassium 4s band to the graphite π^* band is 0.6 according to a self-consistent calculation by Ohno *et al.*[35] When hydrogen is introduced into C_8K [Fig. 8(b)], the center of gravity of the 1s band is located below the Fermi level of C_8K since the strong electron affinity of hydrogen induces charge transfer from C_8K to hydrogen. The NMR experimental result showing the existence of small concentration of carriers on the hydrogen site gives evidence that the top of the band associated with the hydrogen 1s level reaches the Fermi level and generates a small vacancy in this band.

E. Relaxation due to localized electron spins

The relaxation component relatively independent of temperature is attributable to diffusion of nuclear spin excitation to localized electron spins. If the nuclear spin diffusion coefficient is represented by D, T_{1l}^{-1} is given by[26]

$$T_{1l}^{-1}=4\pi NbD \ , \tag{16}$$

and

$$D=\frac{a^2}{30T_2} \ , \tag{17}$$

where a is the internuclear distance between the neighboring nuclei. The quantity N is the number of electron spins per unit volume, and b is the so-called pseudopotential radius[36] of the individual electron spin represented by

$$b=\frac{\pi}{4\sqrt{2}[\Gamma(\frac{5}{4})]^2}\left[\frac{3A'}{10D}\frac{\tau_e}{1+\omega_0^2\tau_e^2}\right]^{1/4} \ , \tag{18}$$

where τ_e is the spin-lattice relaxation time of the electron spin, and ω_0 is the Larmor frequency of a proton. If τ_e is dominated by the direct phonon process, τ_e^{-1} is expected to be small compared with ω_0, and is proportional to temperature and the square of ω_0.[26] This leads to a prediction that T_{1l}^{-1} is independent of ω_0, and is proportional to $T^{1/4}$, which coincides with the experimental observation that T_{1l}^{-1} is almost independent of frequency and temperature. By applying the experimental values of T_{1l}^{-1} and T_2^{-1} and the S spin concentration obtained in Sec. III D, one can conclude from Eqs. (16)–(18) that τ_e is of the order of 100 ms, which is a reasonable value for the direct process.

IV. SUMMARY

A broad proton NMR line was observed in a potassium-hydrogen-graphite ternary intercalation compound, $C_8KH_{0.55}$. The intrinsic linewidth of the spin packet was, however, observed in spin echo envelope, and was explained by assuming regular two-dimensional arrangements of hydride ions. It was shown that the inhomogeneous broadening is possibly attributable to localized electron spins which are expected to be generated at defects associated with excess ($x>0.5$) hydrogen atoms. The electron spin concentration was estimated to be 200–300 ppm relative to the number of protons. It was suggested that the apparently inconsistent NMR results obtained in several different laboratories are caused by difference in concentrations of localized electron spins depending on the character of the host graphite, the hydrogen content, and the conditions of preparation.

The spin-lattice relaxation rate was divided into two terms: a metallic term and the term due to localized electron spins. Analysis of the metallic relaxation component revealed the existence of a small concentration of charge carriers on the hydrogen site. The local density of states at the Fermi level at the hydrogen site was estimated to be $N_H(E_F)=0.014$ states eV^{-1} per spin per atom of hydrogen. This finding shows the weakly metallic nature of hydrogen in a potassium-hydrogen-graphite ternary intercalation compound, different from the strongly metallic nature of hydrogen in transition-metal hydrides, which are regarded as metal-hydrogen alloys. The origin of this weak metallicity is explained by a model in which the energy band associated with hydrogen 1s orbital is almost filled by electrons, but the top of the band reaches the Fermi level, generating a small hole in the band. Comparison of the local density of states at the site of hydrogen, $N_H(E_F)$, with the total density of states derived from electronic specific heat measurement shows that this weak metallicity of hydrogen plays quite a minor part in the carrier transport in $C_8KH_{0.55}$. The majority of the carriers are associated with the graphite π^* band. This picture is consistent with the recent experiment on thermoelectric power in which a small hole band was shown to coexist with a large electron band.

ACKNOWLEDGMENTS

The authors are grateful to Mr. N. Okada for construction of the cryostat. We thank Dr. M. Kobayashi for kindly showing us the magnetic susceptibility data of Grafoil prior to publication. We also thank Professor M. S. Dresselhaus for her discussion on this work. This work was supported in part by the Joint Studies Program (1984–85) of the Institute for Molecular Science, and also by the Grant-in-Aid for Scientific Research No. 61540250 from the Ministry of Education, Science, and Culture, Japan.

[1]D. Saehr and A. Herold, Bull. Soc. Chim. Fr. 3130 (1965).
[2]M. Colin and A. Herold, Bull. Soc. Chim. Fr. 1982 (1971).
[3]P. Lagrange, A. Metrot, and A. Herold, C. R. Acad. Sci. Paris, Ser. C **278**, 701 (1974).
[4]D. Guerard, P. Lagrange, and A. Herold, Mater. Sci. Eng. **31**, 29 (1977).
[5]G. Furdin, P. Lagrange, A. Herold, and C. Zeller, C. R. Acad. Sci. Paris, Ser. C **282**, 563 (1976).
[6]P. Lagrange and A. Herold, Carbon **16**, 235 (1978).
[7]L. Salamanca-Riba, N.-C. Yeh, M. S. Dresselhaus, M. Endo, and T. Enoki, J. Mater. Res. **1**, 177 (1986).
[8]J. Conard, J. Estrade-Szwarckopf, P. Lauginie, M. El Makrini, P. Lagrange, and D. Guerard, Synth. Met. **2**, 261 (1980); J. Conard, H. Estrade-Szwarckopf, P. Lauginie, M. El Makrini, P. Lagrange, and D. Guerard, Physica B+C **105B**, 290 (1981).

[9]T. Enoki, H. Inokuchi, and M. Sano, Chem. Phys. Lett. **86**, 285 (1982).
[10]T. Enoki, M. Sano, and H. Inokuchi, J. Chem. Phys. **78**, 2017 (1983).
[11]H. Murakami, M. Sano, I. Kanazawa, T. Enoki, T. Kurihara, Y. Sakurai, and H. Inokuchi, J. Chem. Phys. **82**, 4728 (1985).
[12]T. Enoki, M. Sano, and H. Inokuchi, Phys. Rev. B **32**, 2497 (1985).
[13]T. Enoki, N.-C. Yeh, S.-T. Chen, and M. S. Dresselhaus, Phys. Rev. B **33**, 1292 (1986).
[14]P. Lagrange, M.-H. Portman, and A. Herold, C. R. Acad. Sci. Paris, Ser. C **283**, 557 (1976).
[15]T. Trewern, R. K. Thomas, G. Naylor, and W. White, J. Chem. Soc. Faraday Trans., Ser. 1, **78**, 2369 (1982).
[16]T. Trewern, R. K. Thomas, and J. W. White, J. Chem. Soc. Faraday Trans., Ser. 1, **78**, 2399 (1982).
[17]S. Kaneiwa, M. Kobayashi, and I. Tsujikawa, J. Phys. Soc. Jpn. **51**, 2375 (1982).
[18]D. E. Nixon and G. S. Parry, J. Phys. D **1**, 291 (1968).
[19]W. G. Clark and J. A. McNeil, Rev. Sci. Instrum. **44**, 844 (1973).
[20]H. Inokuchi, N. Wakayama, T. Kondow, and Y. Mori, J. Chem. Phys. **46**, 837 (1967).
[21]T. Kondow and U. Mizutani, Synth. Met. **6**, 141 (1983).
[22]L. Pauling, *The Nature of the Chemical Bond*, 3rd ed. (Cornell University Press, Ithaca, New York, 1960), Chap. 13.
[23]D. Guerard, N. E. Elalem, C. Takoudjou, and F. Rousseaux, Synth. Met. **12**, 195 (1985).
[24]W. A. Kamitakahara, G. Doll, and P. C. Eklund (unpublished).
[25]I. J. Lowe and R. E. Norberg, Phys. Rev. **107**, 46 (1957).
[26]A. Abragam, *The Principles of Nuclear Magnetism* (Clarendon, Oxford, 1963), Chaps. IV and IX.
[27]J. H. Van Vleck, Phys. Rev. **74**, 1168 (1948).
[28]K. Nomura, T. Saito, K. Kume, and H. Suematsu, Solid State Commun. **63**, 1059 (1987).
[29]M. Kobayashi (private communication).
[30]S. Kazama and Y. Fukai, J. Phys. Soc. Jpn. **42**, 119 (1977).
[31]C. Korn, Phys. Rev. B **17**, 1707 (1978).
[32]C. P. Slichter, *Principles of Magnetic Resonance*, 2nd ed. (Springer-Verlag, Berlin 1978), Chap. 5.
[33]T. Enoki, K. Imaeda, H. Inokuchi, and M. Sano, Phys. Rev. B **35**, 9399 (1987).
[34]E. Clementi and D. L. Raimondi, J. Chem. Phys. **38**, 2686 (1963).
[35]T. Ohno, K. Nakao, and H. Kamimura, J. Phys. Soc. Jpn. **47**, 1125 (1979).
[36]P. G. de Gennes, J. Phys. Chem. Solids **7**, 345 (1958).